



**HAL**  
open science

# A discussion on Darcy-scale modeling of porous media dissolution in homogeneous and heterogeneous systems

F. Golfier, B. Bazin, Didier Lasseux, R. Lenormand, M. Quintard

► **To cite this version:**

F. Golfier, B. Bazin, Didier Lasseux, R. Lenormand, M. Quintard. A discussion on Darcy-scale modeling of porous media dissolution in homogeneous and heterogeneous systems. Computational Methods in Water Resources, Proceedings of the XIVth International Conference on Computational Methods in Water Resources (CMWR XIV), 47, Elsevier, pp.615-622, 2002, Developments in Water Science, 10.1016/S0167-5648(02)80116-2 . hal-03827917

**HAL Id: hal-03827917**

**<https://hal.science/hal-03827917>**

Submitted on 24 Oct 2022

**HAL** is a multi-disciplinary open access archive for the deposit and dissemination of scientific research documents, whether they are published or not. The documents may come from teaching and research institutions in France or abroad, or from public or private research centers.

L'archive ouverte pluridisciplinaire **HAL**, est destinée au dépôt et à la diffusion de documents scientifiques de niveau recherche, publiés ou non, émanant des établissements d'enseignement et de recherche français ou étrangers, des laboratoires publics ou privés.

## A discussion on Darcy-scale modeling of porous media dissolution in homogeneous and heterogeneous systems

F. Golfier<sup>a,b</sup>, B. Bazin<sup>b</sup>, D. Lasseux<sup>c</sup>, R. Lenormand<sup>b</sup> and M. Quintard<sup>a</sup>

<sup>a</sup>Institut de Mécanique des Fluides, allée Camille Soula, 31400 Toulouse, France

<sup>b</sup>Institut Français du Pétrole, 1 et 4 avenue de Bois-Préau,  
92852 Rueil Malmaison Cedex, France

<sup>c</sup>LEPT-ENSAM, esplanade des Arts et Métiers – 33405 Talence Cedex, France

The unstable dissolution of a porous medium leads to complex patterns which are difficult to model quantitatively. A Darcy-scale dissolution model is proposed involving a local non-equilibrium dissolution equation. A 3D numerical model has been developed to solve for the resulting PDEs using an operator splitting technique and high resolution TVD schemes. Results are shown for 2D and 3D configurations for both homogeneous and heterogeneous systems. The qualitative and quantitative features of the numerical results are discussed with respect to the published literature.

Based on the 2D results, a first attempt is made at deriving a core-scale dissolution model based on cross-sectional averages. Several possibilities are explored including one-equation models, i.e., the core-scale medium incorporates the *wormholes* and the remaining porous matrix, and two-equation models for which the *wormholes* are treated separately. Theoretical implications are discussed based on numerical experiments.

### 1 INTRODUCTION

Dissolution mechanism in porous media is frequently encountered in several domains: stimulation of petroleum wells by acid injection to increase the rock permeability<sup>1</sup>, NAPL transport in hydrogeology<sup>2</sup>, or raising the ground level of the Dutch coast by sulfuric acid injection into subsurface limestones<sup>3</sup>. This dissolution process is coupled with the fluid momentum equation in an unstable way: flow velocity is higher in the largest pores, which in generally produces faster dissolution processes. These processes increase locally the pore diameter and this may in turn facilitate the acid transport to these large pores. These physical mechanisms can lead to the formation of highly conductive flow channels called *wormholes*. As a consequence, prediction of wormhole propagation and the understanding of dissolution regimes present a major interest to optimize acidizing treatments. However, the description of dissolution macroscopic patterns is a very complex problem, determined by the flow microscopic characteristics, and with many factors in play such as the injection rate, the acid volume, and rock permeability.

At the pore-scale, the dissolution mechanism involves acid transport by diffusion and advection to the solid surface, chemical reaction at the surface and product transport away from the surface. If the chemical reaction characteristic time is very short compared to the mass-transfer kinetics, the reaction is called *mass-transfer-limited*, and this is generally the

case for limestone dissolution with HCl. On the other side, if mass-transfer kinetics is slow, then the reaction is *reaction-rate limited*, and this is the case for dolomite dissolution at the room temperature.

Several experiments of dissolution have been performed in a variety of fluid-mineral systems, for mass transfer limited as well as reaction-rate limited processes. Hoefner et al.<sup>4</sup> and Fredd et al.<sup>5</sup> used limestone core samples and HCl injection. The wormhole structure is visualized by injecting a low melting point alloy and then dissolving the porous medium or by neutron radiography. In addition to HCl-limestone systems, Several researchers<sup>6,7</sup> investigated the effect of temperature, acid concentration, rock mineralogy and injection rate for some Indiana or Glenn Rose limestone and dolomite cores. All the experiments led to the observation of similar dissolution regimes: face dissolution, conical wormhole, dominant wormhole, ramified wormholes and uniform dissolution. Another result is the existence of an optimum injection rate<sup>4,6</sup>. It corresponds to the maximum penetration of the wormhole for a given volume of acid injected. It is reported that the optimum conditions are related to the formation of a dominant wormhole with little branching through the core. The optimum flow rate depends on several parameters, including the rock mineralogy (calcite or dolomite for carbonate formations), the temperature and the acid concentration.

In order to predict this optimum injection rate and the wormhole development at the Darcy-scale, several numerical models have been developed. Among the different approaches found in the literature, we can distinguish : the network models<sup>4,5</sup> which consider the dissolution of the solid grains in a two or three dimensional structure at the pore-scale, or the capillary tube model<sup>6</sup>, based on a pre-existing shape of the wormhole. We can also cite the dimensionless approach<sup>5,8</sup> based on correlations at the scale of the core sample itself, or the model of Liu et al.<sup>9</sup> which was a first attempt to develop a macroscopic dissolution model. The reader can refer to the paper by Fredd et al.<sup>10</sup> for a detailed presentation of these different models.

Nevertheless, since none of these models could describe all the features of the dissolution physics, in particular they failed to describe the coupled nature of flow and reaction without assuming a wormhole geometry, a macroscopic acid-transport model has been implemented based on a macro-scale description involving a non-equilibrium mass balance model<sup>11,12</sup>. Concerning the momentum equation, assuming that the velocity of the pore-scale interfaces is small enough, we have adopted a Darcy-Brinkman formulation which allows to simulate correctly the flow in the fluid or porous zones in a continuous manner<sup>13</sup>. The effect of dissolution history on the effective properties, such as the permeability, is approximated by direct relationships between the macro-scale parameters. For instance, a direct relationship is adopted between the permeability and the porosity, which is a classical assumption made in geochemistry. We will present in this paper *original* results obtained by this model for both homogeneous and heterogeneous systems and for 2D and 3D configurations. Finally, we will use the 2D results to discuss the possible features of a core-scale dissolution model.

## 2 PRESENTATION OF THE DARCY-SCALE MODEL

The dissolution macroscopic equations can be obtained from the coupled equations of flow and species transport at the pore-scale, and this lead to a local non-equilibrium dissolution problem. Most of the theoretical questions associated with this development have been discussed in Quintard et al.<sup>14</sup>.

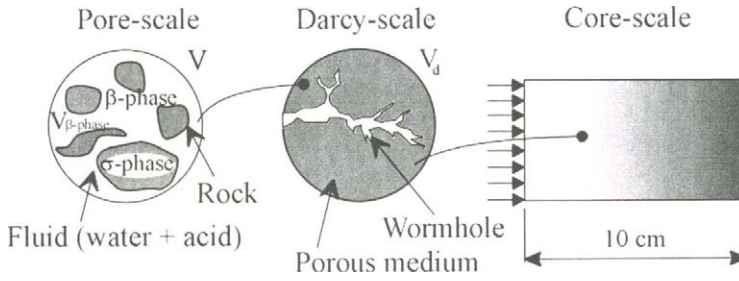


Figure 1. Different scales of the problem.

We just recall below the Darcy-scale model we have used and some of the various results that have been obtained. The solid phase and the fluid phase are identified as the  $\sigma$ -phase and the  $\beta$ -phase respectively. In order to be clear about the equations we have used, we will follow the notations associated with the volume averaging theory presented in Quintard et al.<sup>14</sup>. For instance the superficial velocity is given by

$$\mathbf{V}_\beta = \langle \mathbf{v}_\beta \rangle = \frac{1}{V} \int_{V_{\beta\text{-phase}}} \mathbf{v}_\beta dV \quad (1)$$

where  $V_{\beta\text{-phase}}$  represents the volume of the  $\beta$ -phase contained within the averaging volume,  $V$ , represented Figure 1. The intrinsic mass concentration is defined by

$$C_{A\beta} = \langle c_{A\beta} \rangle^\beta = \frac{1}{V_{\beta\text{-phase}}} \int_{V_{\beta\text{-phase}}} c_{A\beta} dV \quad (2)$$

and we have a similar definition for the intrinsic pressure. We consider that the reaction is *mass-transfer limited*, and the acid is immediately consumed as soon as it reacts with the solid surface. Additional convective terms which appear during the upscaling are neglected. By this way, we obtain a complete system of equations which combines a Darcy-Brinkman model for the flow description in both zones (fluid and porous region) with a local non-equilibrium dissolution model. It can be written under dimensionless form as follows

#### Flow equations:

$$\frac{\mu}{\varepsilon_\beta} \Delta \mathbf{V}_\beta - \nabla P_\beta - \mu \mathbf{K}^{-1} \cdot \mathbf{V}_\beta = 0 \quad (3)$$

where  $\mu$  is the viscosity,  $\mathbf{K}$  and  $\varepsilon_\beta$  are the permeability tensor and the porosity respectively. This equation is coupled with the overall mass balance equation for the fluid phase which may be approximated by

$$\nabla \cdot \mathbf{V}_\beta = 0 \quad (4)$$

### Species transport equations :

$$\varepsilon_{\beta} \frac{\partial C_{A\beta}}{\partial t} + \mathbf{V}_{\beta} \cdot \nabla C_{A\beta} = \nabla \cdot (\mathbf{D}^* \cdot \nabla C_{A\beta}) - \alpha C_{A\beta} \quad (5)$$

$$\frac{\partial \varepsilon_{\beta}}{\partial t} = \frac{\beta \alpha C_{A\beta}}{\rho_{\sigma}} \quad (6)$$

where  $\beta$  represents the stoichiometric coefficient of the chemical reaction. The mass transfer coefficient  $\alpha$  and the dispersion tensor  $\mathbf{D}^*$  are calculated from closure problems<sup>14</sup>. A numerical model has been developed to solve these equations<sup>11</sup>. Given the different mechanisms involved, the numerical model uses a multiple-step approach. First, the stationary Darcy-Brinkman problem is solved for a given porosity field by a predictor-corrector method coupled with an Uzawa algorithm. The effective coefficients in the transport equations are obtained previous to the simulation as a function of the porosity and velocity field by numerically solving on a *representative periodic unit cell* the pore-scale closure problems presented in Golfier et al.<sup>11</sup>. The acid concentration profile resulting from the transport equation can be used to solve for the dissolution equation, Eq. (6). This will eventually lead to a new porosity field which will be used in the next iteration. In practice, the permeability field is directly obtained from the porosity field, by the use of a classical Kozeny-Carman relation  $\mathbf{K} - \varepsilon_{\beta}$ . This particular choice is not a constraint of the model, and other correlations can be used. Various calculations have been performed on two-dimensional and three-dimensional domains, and the different results are discussed in the next section.

## 3 RESULTS AND DISCUSSION

### 3.1 Homogeneous system

In a recent paper<sup>11</sup> we have shown that the simulations allow to capture the different dissolution regimes for “Darcy-scale homogeneous systems”. We can see in Figure 2 the different 2D dissolution figures obtained numerically for different acid injection rates. All these figures represent the porosity field. The obtained dissolution patterns are remarkably equivalent to the experimental dissolution patterns obtained for calcite dissolution<sup>5,10</sup> or for water/salt system<sup>11</sup>. These results allowed us to study in some details the transitions between the different regimes in terms of behavior diagrams. In addition, the performed simulations have shown the existence of an *optimum injection rate*<sup>11</sup>, similarly to the experimental results. This proves the potential of the proposed model. New results are presented in the sequel of the paper to illustrate this potential.

First, the model can be used to obtain 3D dissolution figures as it is illustrated in Figure 3. To our knowledge, none of the existing models can actually capture the wormholing phenomenon in three dimensions. The only attempt made with the PRN *network* model<sup>5</sup>, was strongly limited by the maximal size of the domain (0.1cm x 0.003 cm<sup>2</sup>).

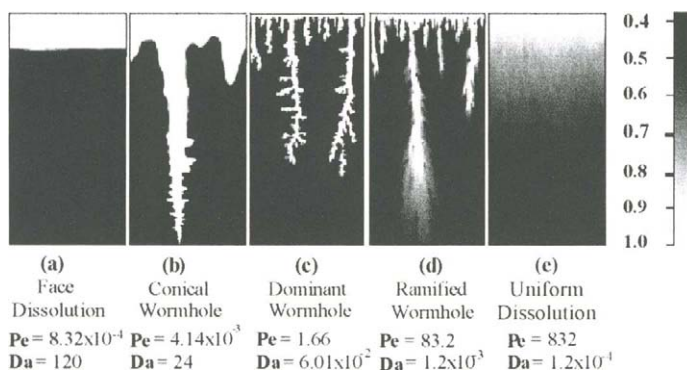


Figure 2. Porosity fields representative of the dissolution patterns (From Golfier et al.<sup>11</sup>).

It must be emphasized here the importance of the choice of the Darcy-Brinkman formulation for the flow model. In fact, we could have used a classical Darcy / Darcy model, which is simpler compared to the Darcy-Brinkman formulation. However, it requires the introduction of an appropriate value for the permeability in the wormhole, i.e., in the *fluid zone* (noted  $K_{\text{fluid}}$  and called fluid permeability). This concept of fluid permeability is artificial and it must be chosen by *a posteriori* arguments to recover the correct physics. For the Darcy-Brinkman model, the fluid permeability needs only to be large enough so that the model leads asymptotically towards the Stokes equation, i.e., the Darcy term vanishes as the porosity is close to one and the fluid permeability does not play any role. On the contrary, with the Darcy-Darcy formulation, the obtained velocity varies with the fluid permeability value. Therefore, an appropriate value of the fluid permeability must be chosen to model correctly the flow into the wormhole. If this value may be estimated in some cases, flow between two parallel plates, for example, this estimation is practically impossible in a 3D flow without assuming a tube geometry for the wormhole.

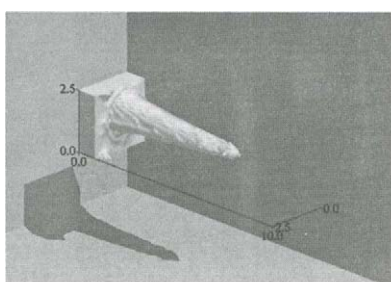


Figure 3. 3D porosity field in conical regime.

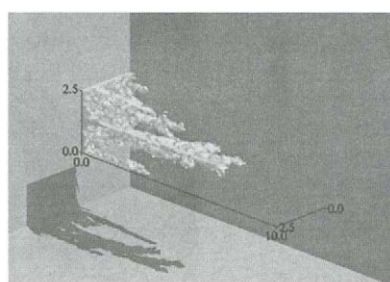


Figure 4. 3D porosity field in wormholing regime.

### 3.2 Heterogeneous systems

Such a model can also be applied easily to heterogeneous systems. We consider a stratified system made of two different porous media of permeability  $K_1 = 10^{-11} \text{ m}^2$  and  $K_2 = 10^{-8} \text{ m}^2$

respectively. We will limit here our study to two simple limit cases : a domain in which the acid solution is injected perpendicularly to the strata and a domain in which the acid solution is injected parallel to the strata. The numerical data for both simulations are given in Table 1.

Table 1  
Numerical data

Constant Flow Rate : $Q = 272 \text{ cm}^3 \cdot \text{h}^{-1}$	
201 x 101 nodes	$C_{A\beta} = 150 \text{ kg} \cdot \text{m}^{-3}$
$\rho_{\sigma} = 2700 \text{ kg} \cdot \text{m}^{-3}$	$\mu = 10^{-3} \text{ Pa} \cdot \text{s}$
$\varepsilon_{\beta} = 0.38$	$\beta = 1.37$
$D^* = 10^{-9} \text{ m}^2 \cdot \text{s}^{-1}$	$\alpha = 10 \text{ s}^{-1}$

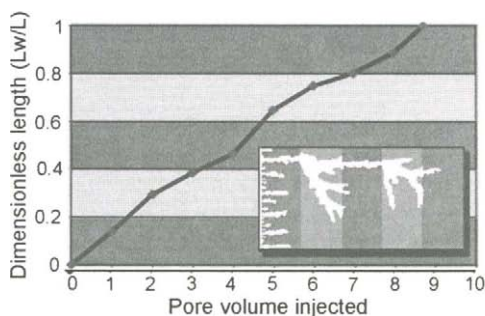


Figure 5. Wormhole length as a function of the pore volume injected and associated dissolution pattern for *strata in series*.

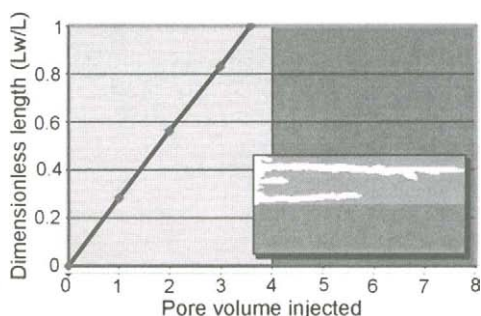


Figure 6. Wormhole length as a function of the pore volume injected and associated dissolution pattern for *strata in parallel*.

The results in Figure 5 shows how complex is the evolution of the unstable dissolution front due to the heterogeneity effects: early stage in one stratum similar to the homogeneous case, then interaction of the dominant wormhole with the second medium, and subsequent complicated evolution, different from the homogeneous case. On the contrary, for the flow parallel to the strata, Figure 6, dissolution occurs essentially in the more permeable region like in the homogeneous case. This illustrates the interest of the proposed model. However, numerical limitations exists, and domain of very large extent are beyond our possibilities. A larger-scale averaged model, or core-scale model (Figure 1), if available, would open new possibilities, and this is the subject of the next section.

#### 4 CORE-SCALE MODELING

In this section, we discuss the introduction of the macroscopic equations which may be used to describe the problem at the core-scale<sup>12</sup>. For the flow description at this scale, a classical Darcy's law is obtained by averaging the Darcy-Brinkman formulation. With regard to the transport and dissolution part, it is not obvious to apply an upscaling method which leads to some core-scale equations valid in a general way. In fact, the value of the mass transfer coefficient can strongly modify the acid transport behavior and the corresponding Darcy-scale dissolution pattern.

*One-equation model.* First, a simple one-equation model can be proposed similar to the Darcy-scale model presented in the previous sections.

$$\varepsilon_{\beta}^* \frac{\partial C_{A\beta}^*}{\partial t} + \mathbf{V}_{\beta}^* \cdot \nabla C_{A\beta}^* = \nabla \cdot (\mathbf{D}^{**} \cdot \nabla C_{A\beta}^*) - \alpha^* C_{A\beta}^* \quad (7)$$

$$\frac{\partial \varepsilon_{\beta}^*}{\partial t} = \frac{\beta \alpha^* C_{A\beta}^*}{\rho_{\eta}} \quad (8)$$

where  $\varepsilon_{\beta}^*$  is the macroscopic porosity,  $\alpha^*$  and  $C_{A\beta}^*$  the core-scale mass transfer coefficient and acid mass concentration respectively. The 1D core-scale velocity is taken as constant.

*Two-equation model.* If the value of the mass transfer coefficient is very important, we obtain two different regions: a fluid region in the dissolved areas, and a porous region where dissolution has not occurred. This looks like a double-porosity system, and this suggests the introduction of a *two-equation model* for which the *wormholes* ( $\varpi$ -region) and the remaining porous matrix ( $\eta$ -region) are treated separately. The transport equations are written as

$$\phi_{\varpi} \frac{\partial C_{A\varpi}^*}{\partial t} + \mathbf{V}_{\varpi}^* \cdot \nabla C_{A\varpi}^* = \nabla \cdot (\mathbf{D}_{\varpi}^{**} \cdot \nabla C_{A\varpi}^*) - \alpha^* C_{A\varpi}^* \text{ in the } \varpi \text{-region} \quad (9)$$

$$\frac{\partial \phi_{\varpi}}{\partial t} = \frac{\beta \alpha^* C_{A\varpi}^*}{\rho_{\sigma}} \text{ in the } \varpi \text{-region} \quad (10)$$

where  $\phi_{\varpi}$  represents the fluid fraction,  $C_{A\varpi}^*$  and  $C_{A\eta}^*$  the core-scale regional acid mass concentrations and  $\mathbf{V}_{\varpi}^*$  the superficial velocity in the  $\varpi$ -region. These equations are completed by  $C_{A\eta}^* = 0$  in the  $\eta$ -region.

The dissolution patterns obtained numerically at the Darcy-scale are used to determine the correlations for the core-scale effective coefficients (macroscopic permeability  $\mathbf{K}^*$ , core-scale mass transfer coefficient  $\alpha^*$ , fluid fraction  $\phi_{\varpi}$  and macroscopic porosity  $\varepsilon_{\beta}^*$ ) by spatial integration. The obtained results show an acceptable independence of these coefficients with respect to the dissolution history at least for certain conditions (wormholing regime in particular, see an example of correlation in Figure 7).

From the system of equations obtained at the core-scale and the mass transfer and permeability correlations provided by the numerical simulations at the Darcy-scale, a 1D core-scale model can be developed for both approaches to verify the validity of such a representation. To check the validity, we compared predictions provided by these core-scale models with direct Darcy-scale simulations. Figure 8 presents the comparison of these simulations for  $Q = 50 \text{ cm}^3 \cdot \text{h}^{-1}$  and  $C_{A\beta} = 545 \text{ kg} \cdot \text{m}^{-3}$ . If the results obtained by the one-equation model are not satisfactory, the two-equation model correctly predicts the wormhole propagation and presents a relatively good agreement with the Darcy-scale model. This suggests that a simple, fickian, dispersive model with chemical reaction is not well suited to model the dissolution of a porous medium at the core-scale in the presence of wormholes. If one is looking at a one-equation model, it must be more complicated. Work is currently undertaken in this direction.



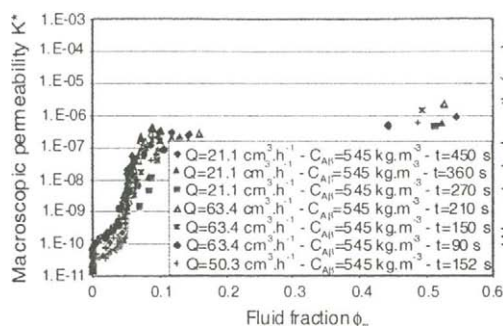


Figure 7.  $K^*$  -  $\phi_w$  correlation in the wormholing regime.

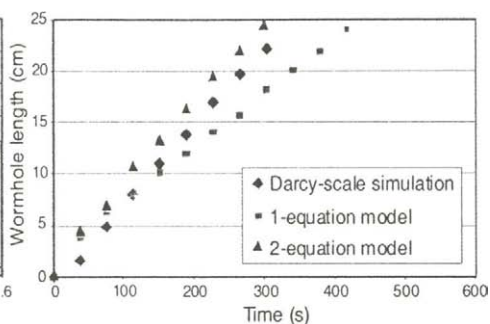


Figure 8. Wormhole length as a function of time for different models.

## 5 CONCLUSION

A three-dimensional Darcy-scale dissolution model has been presented in this paper. Its originality lies in the fact that it is based on a combination of a Darcy-Brinkman model coupled with a local non-equilibrium dissolution model. Simulations have been performed for 2D and 3D configurations for both homogeneous and heterogeneous systems and present a good agreement with the literature. Based on the 2D results, different approaches have been explored to model dissolution phenomena at the core-scale. A double-porosity model has shown a relatively good agreement with the direct simulations, at least under local equilibrium conditions, compared to a simple one-equation model. This indicates that complicated dynamic effects are present which may require the use of a more complex one-equation model. Developments are made in this direction.

## REFERENCES

1. G. Rowan, (1959), J. Inst. Petrol. 45(431).
2. S.E. Power, L.M. Abriola and W.J. Weber, (1992), Water Resour. Res. 28(10), 2691-2705.
3. R. Schuiling, (1990), Appl. Geochem. 5, 251-262.
4. M.L. Hoefner and H.S. Fogler, (1988), AIChE J. 34(1), 45-54.
5. C.N. Fredd and H.S. Fogler, (1998), AIChE, J. 44(9), 1933-1949.
6. Y. Wang, A.D. Hill and R.S. Schechter, (1993), SPE 26578, Tech. Conf. and Exhib., Houston.
7. B. Bazin, Roque, C. & Bouteica, M. (1995), SPE 30085, Europ. Dam. Conf., The Hague.
8. G. Daccord, R. Lenormand and O. Lietard, (1993), Chem. Engng. Sci. 48(1), 169-178.
9. X. Liu, A. Ormond, K. Bartko, Y. Li, Y. and P. Ortoleva, (1997), J. of Petrol. Sci. and Engng 17, 181-196.
10. C.N. Fredd, and M.J. Miller, (2000), SPE 58713, Int. Symposium on Formation Damage, Lafayette, Louisiana.
11. F. Golfier,, C. Zarcone, B. Bazin, R. Lenormand,,D. Lasseux, and M. Quintard, (2002), J. Fluid Mech., in press.
12. F. Golfier, (2001), PhD Thesis, INP Toulouse.
13. C. Beckermann, R. Viskanta and S. Ramadhyani, (1988), J. Fluid Mech. 186, 257-284.
14. M. Quintard and S. Whitaker, (1999), Ind. and Engng Chem. Res. 38(3), 833-844.